Design and Analysis of CubeSat Microwave Radiometer Constellations to Observe Temporal Variability of the Atmosphere

Yuriy V. Goncharenko, *Member, IEEE*, Wesley Berg, *Member, IEEE*, Steven C. Reising, *Senior Member, IEEE*, Flavio Iturbide-Sanchez, *Senior Member, IEEE*, and V. Chandrasekar, *Fellow, IEEE*

***Abstract*—Passive microwave satellite observations provide critical information for global forecast models, particularly in cloudy and/or precipitating conditions. The limited temporal sampling provided by current operational polar orbiters cannot capture rapidly changing conditions such as the development of convective storms. This is a significant issue for open-ocean weather systems such as tropical cyclones and hurricanes that can only be effectively monitored from satellites. The recent development and demonstration of miniaturized microwave radiometers on-board low-cost CubeSat satellites has the potential to dramatically improve the temporal and spatial sampling of all-sky microwave observations by deploying a substantial constellation of satellites in low Earth orbit. Two constellations of 60 CubeSats in 550 km orbits are compared to the current operational microwave sensors. One approach employs all polar orbiters, while the other approach uses multiple inclination orbits for increased sampling over convective storm regions. Both approaches reduce average revisit times to approximately 20–30 min globally, and the multi-inclination approach also provides irregular 5–10 min sampling over selected latitudes. Improved global temporal sampling would provide all-sky observations to global forecast models over rapidly changing environments, while millimeter-wave observations over convective storm regions would be valuable for both forecasting and studying the development of convective storms. This article demonstrated that a constellation of low-cost CubeSats with microwave radiometers has the potential to provide equivalent temporal resolution to that observed from sensors on geostationary orbit.**

***Index Terms*—Passive microwave remote sensing, radiometers, satellite constellations.**

I. Introduction

RECENT technological advances have enabled the development of small and low-cost satellites capable of providing science-quality passive microwave observations from low Earth orbit (LEO), with similar capabilities to existing operational sensors. The development of these low-cost satellites and sensors makes possible the deployment of a constellation of satellites capable of providing greatly enhanced temporal sampling on a global basis. While current operational microwave sensors are limited to two different LEO orbits, and therefore a maximum of four observations per day for a given location, the dramatically lower cost of CubeSat satellites has the potential to provide much more frequent temporal sampling for improved global forecasting and hurricane/storm monitoring applications.

A number of CubeSat satellites with microwave radiometers have already demonstrated the capability of this new technology for Earth observations from LEO [1], [2]. The first CubeSat mission to provide multifrequency microwave brightness temperatures for Earth observations on a global basis is the Temporal Experiment for Storms and Tropical Systems–Demonstration (TEMPEST-D). TEMPEST-D is a 6U CubeSat technology demonstration satellite with a cross-track millimeter-wave radiometer measuring at five frequencies from 87 to 181 GHz [3]. The 87 GHz observations are sensitive to both the surface and water vapor in the lower troposphere, and the four frequencies from 164 to 181 GHz provide water vapor profiling information using the pressure broadening of the 183.31 GHz absorption line. TEMPEST-D was deployed into orbit from the International Space Station (ISS) on July 13, 2018 and has been operated for nearly three years. On-orbit validation of the calibrated TEMPEST-D brightness temperatures indicates that it has comparable or better performance in terms of instrument noise, calibration accuracy, and calibration stability than similar operational radiometers such as the microwave humidity sounder (MHS) [4].

The TEMPEST concept takes advantage of low-cost microwave sensors on CubeSats for a potential constellation to provide frequent observation of rapid-evolving storms and the surrounding water vapor environment. Using a similar concept, the Time-Resolved Observations of Precipitation structure and storm Intensity with a Constellation of CubeSats (TROPICS) is a NASA Earth Venture science mission that is planned for launch in 2022. TROPICS will consist of six 3U CubeSats in three orbital planes, each with a 12-channel microwave/millimeter-wave radiometer, to demonstrate the capability of a small constellation of CubeSats to improve temporal sampling over the tropics ($\pm$ 30° latitude) [5].

The current constellation of operational sensors providing global microwave observations consists of the Advanced Technology Microwave Sounder (ATMS) on board

Manuscript received June 7, 2021; revised October 12, 2021; accepted October 31, 2021. Date of publication November 15, 2021; date of current version December 1, 2021. This work was supported in part by the NOAA/NESDIS/OSAAP under Grant 1332KP20CNEEP0085 to Colorado State University, and in part by the NASA SMD/ESD under Grants NNX15AP56G and 80NSSC20K1124 to Colorado State University. *(Corresponding author: Yuriy V. Goncharenko.)*

Yuriy V. Goncharenko, Steven C. Reising, and V. Chandrasekar are with the Department of Electrical and Computer Engineering, Colorado State University, Fort Collins, CO 80523 USA (e-mail: yuriy.goncharenko@colostate.edu; steven.reising@colostate.edu; chandra@colostate.edu).

Wesley Berg is with the Department of Atmospheric Science, Colorado State University, Fort Collins, CO 80523 USA (e-mail: berg@atmos.colostate.edu).

Flavio Iturbide-Sanchez is with the Center for Satellite Applications and Research, National Environmental Satellite, Data, and Information Service, National Oceanic and Atmospheric Administration, College Park, MD 20740 USA (e-mail: flavio.iturbide@noaa.gov).

Digital Object Identifier 10.1109/JSTARS.2021.3128069

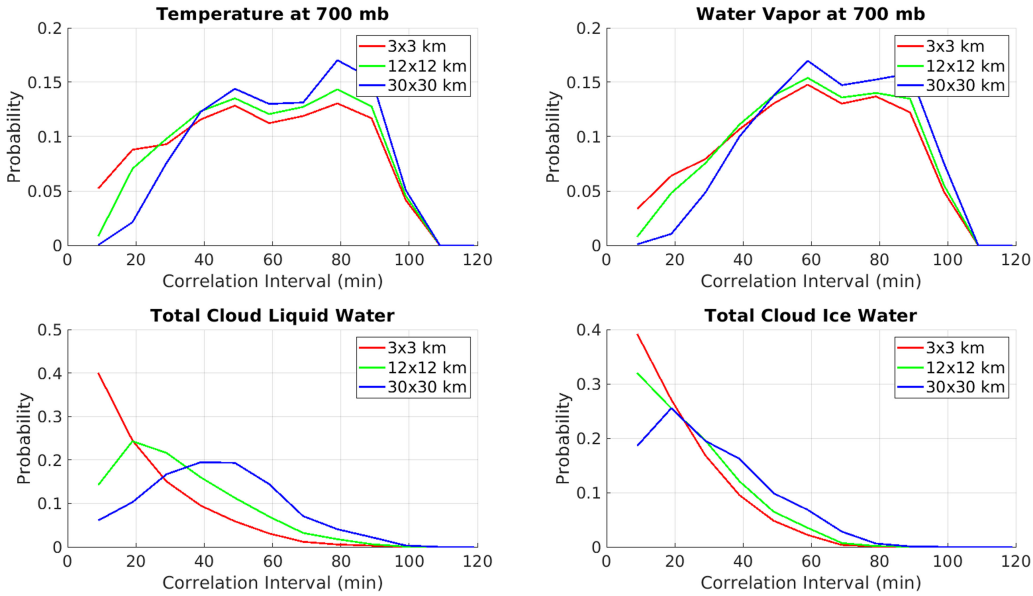

Fig. 1. Probability density functions (PDFs) of correlation intervals. (Upper left): PDF of temperature at 700 mb isobar pressure altitude. (Upper right): PDF of water vapor mixing ratio at the same altitude. (Lower left): PDF of total cloud liquid water content. (Lower right): PDF of total cloud ice water content. For all plots, the red, green, and blue curves represent PDFs for footprint sizes of 3×3, 12×12, and 30×30 km, respectively.

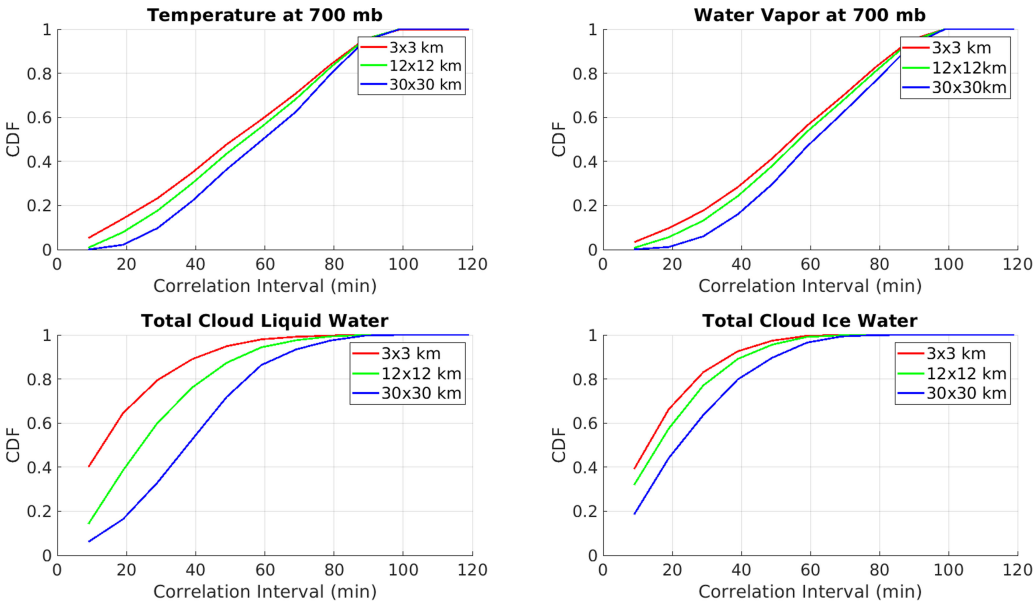

Fig. 2. Cumulative distribution functions (CDFs) of correlation intervals. (Upper left): CDF of temperature at 700 mb isobar pressure altitude. (Upper right): CDF of water vapor mixing ratio at the same altitude. (Lower left): CDF of total cloud liquid water content. (Lower right): CDF of total cloud ice water content. For all plots, the red, green, and blue curves represent PDFs for footprint sizes of 3×3, 12×12, and 30×30 km, respectively.

the Suomi National Polar-orbiting Partnership and NOAA-20 satellites, and the AMSU-A and MHS instruments on board the ESA/EUMETSAT MetOp-A/B/C satellites. These satellites are in polar sun-synchronous orbits with the NOAA satellites providing observations near 1:30 am/pm local time and the MetOp satellites providing observations near 9:30 am/pm local time. This provides a total of four observations per day over most of the globe with gaps between subsequent observations ranging from approximately 4 to 10 h. While this is generally adequate for tracking changes in large-scale temperature and water vapor fields in clear-sky or nonprecipitating conditions, it lacks the capability to observe the changes associated with convective storm cells, which typically develop on a time scale of a few hours or less. While geostationary visible and infrared observations can provide frequent updates on the location, shape and horizontal extent of hurricanes, typhoons, and tropical cyclones, they are limited to observing cloud-top properties and cannot detect changes internal to the clouds (or, of course, the underlying sea surface properties) that might lead to rapid intensification. In contrast, microwave observations can provide information on cloud microphysical properties internal to a storm, but are presently limited by their much lower temporal

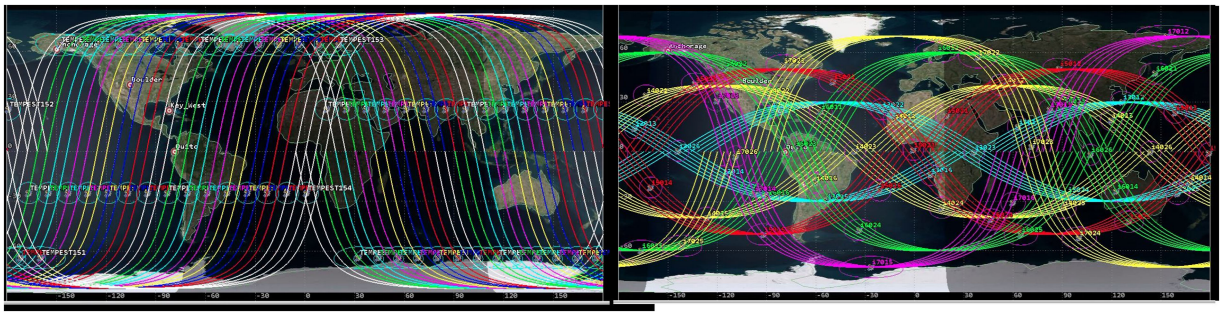

Fig. 3. Simulated ground tracks of (a) TEMPEST Polar constellation and (b) TEMPEST MIC constellation over a single orbital period (i.e., approximately 95 min).

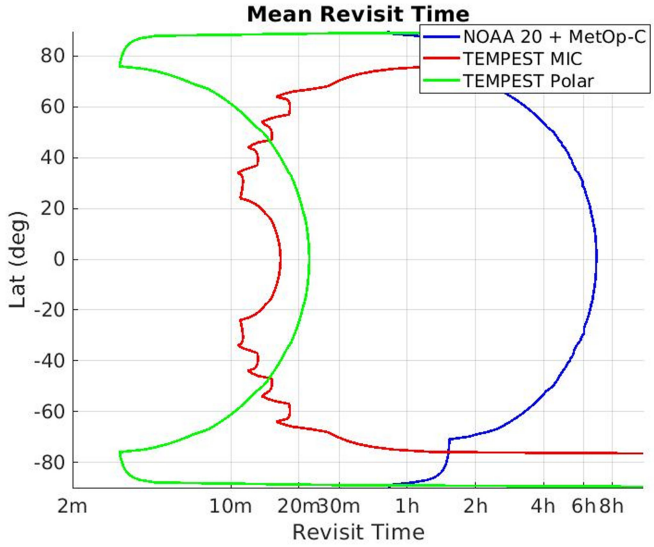

Fig. 4. Mean revisit time for the NOAA-20/MetOp-C polar orbiters (blue), the TEMPEST MIC (red), and TEMPEST Polar (green) constellations. On the horizontal axis labels, "m" indicates the revisit time in minutes, and "h" in hours.

sampling and spatial resolution. Deploying a constellation of low-cost CubeSat radiometers to provide frequent microwave observations has great potential for improving forecasts and many other atmospheric science applications.

Designing a constellation to provide improved temporal sampling with global coverage involves a number of tradeoffs. The purpose of the simulation results presented in this article is to provide the reader with a sense of how microwave observations from a constellation of low-cost CubeSat satellites could provide dramatically improved temporal sampling for both global forecasting and storm tracking applications. Considering the substantially lower cost of a CubeSat compared to current operational satellites, we chose to simulate two different constellation configurations with a total of 60 satellites each. While this may seem like a large number of satellites, private companies like SpaceX are already deploying thousands of CubeSats into orbit. There are also a number of smaller constellations such as Spire Global (90 satellites [6], [7]) or BlackSky (up to 60 satellites [8]), which shows the feasibility of designing such constellations with current technology. Considering the dramatically lower cost of CubeSats along with the availability of low-cost launch options, we feel this is a realistic goal in the near future.

A significant tradeoff in the design of a CubeSat constellation involves spatial resolution versus temporal sampling. A higher orbit results in a wider observation swath and therefore improved temporal sampling, but it also decreases the spatial resolution of the sensor. To provide reasonably high spatial resolution in order to sample changes in storm systems such as hurricanes or tropical cyclones, we propose to use a 12U CubeSat (twice the volume of the actual TEMPEST-D 6U CubeSat). This approach enables an improvement in the spatial resolution by doubling the size of the antenna. The four water vapor profiling frequency channels on TEMPEST-D have a spatial resolution of 12.5 km. Because the TEMPEST-D CubeSat was deployed from the ISS, the mission operated from an initial orbital altitude of 405 km. This worked well, since the TEMPEST-D mission is in a period with low solar activity (2018–2021), but it could lead to a relatively short lifetime and potential attitude control issues in a period with high solar activity. Therefore, these simulations were conducted using a slightly higher but still relatively low orbital altitude of 550 km. The larger antenna afforded by the 12U spacecraft bus combined with a 550 km orbital altitude provides a spatial resolution of approximately 9 km for the four TEMPEST-D frequency channels near the 183.31 GHz water vapor absorption line.

II. Methodology Overview

An important consideration in the design of a satellite constellation to provide observations for global weather forecasting is the revisit time between subsequent observations. Long gaps between subsequent revisits, as is the case for the current polar constellation with only two different LEO orbits, at times miss rapid changes in atmospheric conditions, resulting in large sampling errors. This is the case for convective activity, in which the life cycle of individual storm cells often lasts for less than a few hours [9]. Achieving rapid revisit times, however, requires a larger number of satellites in a constellation, thereby increasing operational complexity and cost.

In this context, Section III of the article is focused on determining an optimal constellation revisit time, which depends on the spatiotemporal variability of the atmospheric parameter to be sampled. This variability in turn depends on the sensor's spatial resolution and the nature of the parameter being observed, which vary both regionally and seasonally.

Once the desired revisit time is estimated, the constellation design analysis is performed, as described in Section IV-A variety of quality metrics can be used to estimate the performance of the constellation. The simplest metric is the mean

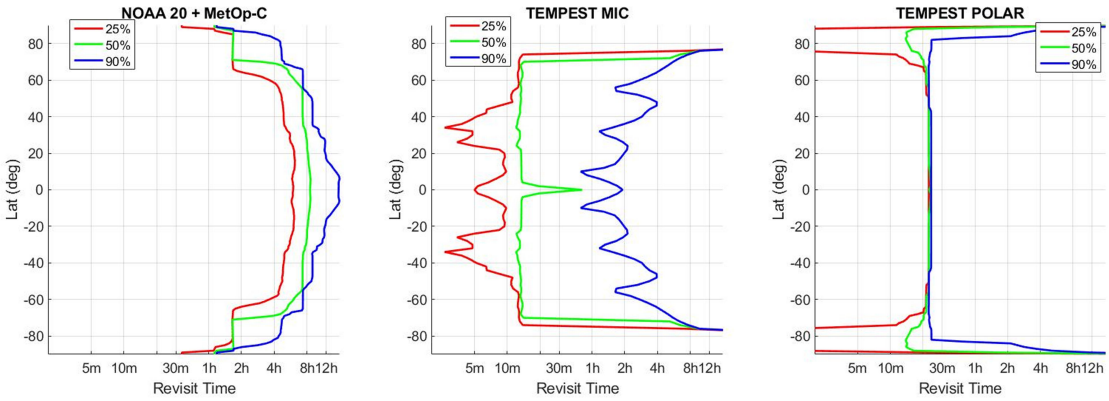

Fig. 5. Revisit time for 25% (red), 50% (green), and 90% (blue) of total observation time (6, 12, and approximately 21.5 h per day, respectively) for current polar orbiters, NOAA 20 and MetOP-C (left), the TEMPEST-MIC (center), and TEMPEST Polar (right) constellations.

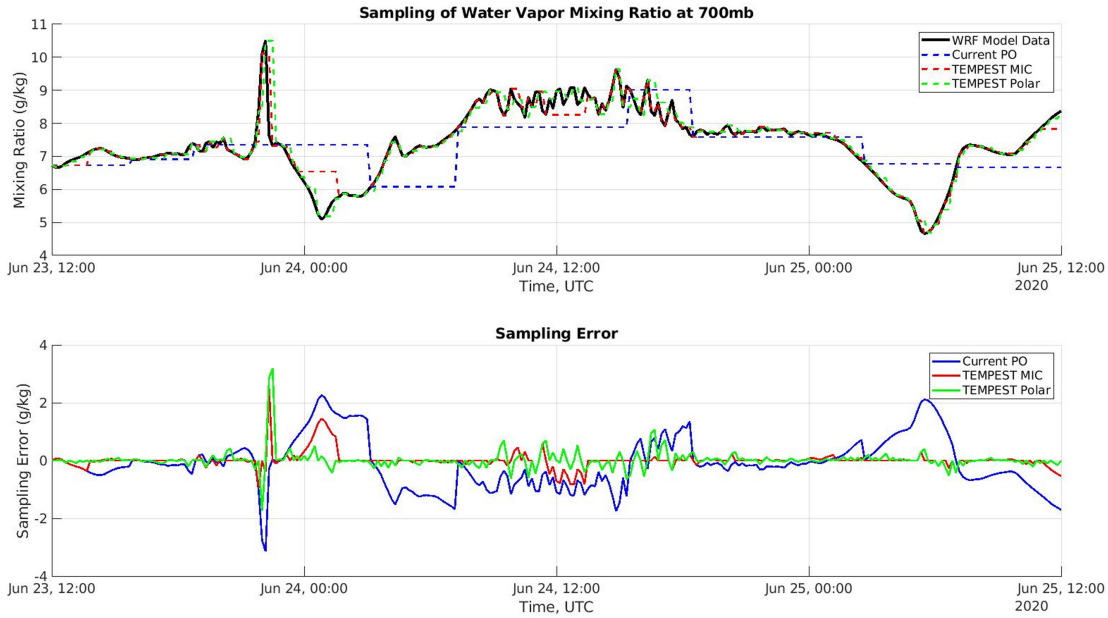

Fig. 6. (Upper panel) Temporal sampling of water vapor mixing ratio at 700 mb pressure altitude at Corpus Christi, TX. (Lower panel) The corresponding temporal representativeness error for the three constellation configurations studied.

revisit time. More complex metrics are based on cumulative distribution function (CDF) analysis. The most straightforward way to compare the performance of a variety of constellation designs is to sample a dynamic atmospheric process, e.g., the development of a convective cell resulting in a thunderstorm. Section IV presents the sampling of such an event simulated using the Weather Research and Forecasting (WRF) Model.

III. Determining Optimal Revisit Time to Observe Atmospheric Variability

A common method to characterize spatiotemporal variability is to evaluate the longest separation in time or space over which the autocorrelation between values of the process is still statistically significant.

This separation is typically referred to as the correlation interval, correlation window, or duration of correlation [10].

Steinke *et al.* [11] performed a simulation within the ICOsahedral Nonhydrostatic modelling framework to study the variability of integrated water vapor (IWV) in spatial and temporal scales of less than 10 km and 1 h, respectively. Their results show that spatial differences of 3–4 km or temporal differences of 10–15 min correspond to changes in IWV on the order of 0.4 kg/m^2. This article also shows that the correlation between simultaneous IWV observations 10 km apart drops to 0.84. A similar decrease in the correlation occurs for collocated measurements separated by $\sim$1 h. Vogelmann *et al.* [12] investigated the spatiotemporal variability of water vapor above the Zugspitze mountain in Germany using a Fourier-transform infrared spectroscopy instrument. A 20-min sampling interval resulted in a standard deviation of the sampling error of 0.15 mm (0.15 kg/m^2) in IWV, which increased to 0.25 mm (0.25 kg/m^2) for a 40-min sampling interval.

For spatiotemporal variability in cloudy atmospheres, Bley *et al.* [13] studied the evolution of warm convective cloud fields

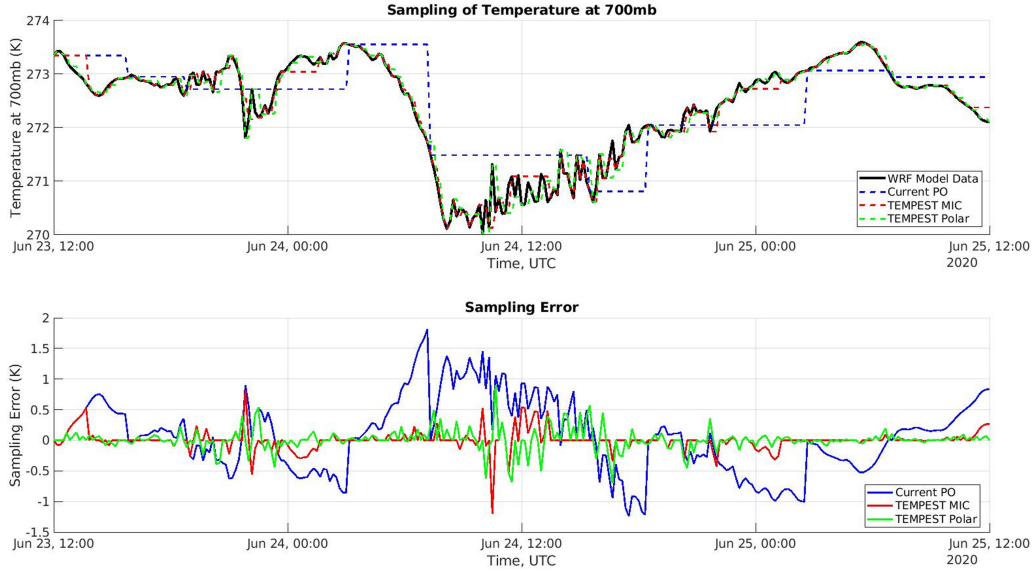

Fig. 7. (Upper panel) Temporal sampling of atmospheric temperature at 700 mb pressure altitude at Corpus Christi, TX. (Lower panel) The corresponding temporal representativeness error for the three constellation configurations studied.

over central Europe based on Meteosat data. They found that the spatial decorrelation length of cloud liquid water path (LWP) varied from 6.5 to 8 km, and the temporal decorrelation interval ranged from 10 to 15 min for a spatial resolution of 21 km^2. These studies provide some insights into the spatiotemporal variability of water vapor and clouds, although they are limited to certain cloud features [13] or regions ([12]) or are focused on intercomparisons among different instruments or between observations and simulations [11].

To further evaluate the spatiotemporal variability of atmospheric parameters over a range of temporal and spatial scales, several weather events occurred over CONUS, including thunderstorms and intense winter storms, were simulated using the WRF Model. The WRF simulations were run using the physics options set as suggested in [14] for 1–4 km grid distances. To initialize the simulations, the NCEP GFS 0.25 Degree Global Forecast Grids Historical Archive data [14] was used. The simulation time step and grid spacing were set to 5 s and 3 km, respectively. To keep the amount of output data reasonable, the temporal resolution of the model output was set to 10 min. This analysis focused on the spatiotemporal variability of the model outputs of atmospheric temperature, water vapor mixing ratio, cloud liquid water, and ice water path (IWP) variables. To analyze the spatiotemporal variability of atmospheric parameters, three output resolution settings were chosen: 3 $\times$ 3 km, corresponding to the resolution of the WRF model output, 12 $\times$ 12 km, corresponding to the approximate spatial resolution of the water vapor profiling channels of the constellation satellites, and 30 $\times$ 30 km, corresponding to the lowest resolution of the 89 GHz channels on ATMS.

Autocorrelation functions of the simulation time series were calculated for all grid points, and the resulting correlation times were analyzed. Probability density functions (PDFs) and CDFs of atmospheric temperature and water vapor mixing ratio at 700 mb pressure altitude, along with total cloud liquid and IWPs, are shown in Figs. 1 and 2, respectively. Fig. 1 shows that the correlation intervals for atmospheric temperature and water vapor mixing ratio at 700 mb pressure altitude vary between 40 and 90 min and do not depend significantly on the spatial resolution. Not surprisingly, cloud LWP and IWP exhibit much higher temporal and spatial variability. PDFs corresponding to a sensor spatial resolution of 3 $\times$ 3 km indicate a correlation interval of less than 10 min for both LWP and IWP. For a sensor spatial resolution of 12 $\times$ 12 km, the correlation interval of LWP increases to 10–30 min and to 30–60 min for a resolution of 30 $\times$ 30 km IWP exhibits even larger variability, with a correlation interval in the range of 10 min or less at finer spatial resolutions, increasing to $\sim$20 min at 30 $\times$ 30 km. The CDFs in Fig. 2 indicate that for 50% of the analyzed area, the correlation intervals for both temperature and water vapor are 60 min or less. Correspondingly, for 50% of the analyzed area covered by clouds, the correlation intervals of LWP and IWP decrease to 10, 25, and 40 min for 3 $\times$ 3, 12 $\times$ 12, and 30 $\times$ 30 km footprints, respectively.

As mentioned previously, the spatiotemporal variability of these atmospheric parameters has a strong seasonal and geographic dependence. As a result, the CDFs and PDFs shown in Figs. 1 and 2 are not necessarily applicable on a global basis. Considering these limitations, however, the results from the WRF simulations are similar to results from the studies in [11]–[14] and are therefore useful guidelines to consider in the design of a satellite constellation. Therefore, to adequately capture the spatiotemporal variability in temperature and water vapor, a mean revisit time on the order of $\sim$1–2 h is needed. For a spatial resolution of 12 $\times$ 12 km, more frequent observations on the order of 20–30 min are needed to capture the development of convective storm systems.

IV. Orbital Configuration for a CubeSat Constellation

To achieve significantly shorter revisit times to capture the spatiotemporal variability discussed above, several options were considered. To keep things manageable, this article focuses on possible configurations with a constellation of up to 60 satellites. Given the constraint of a fixed number of satellites, one possible

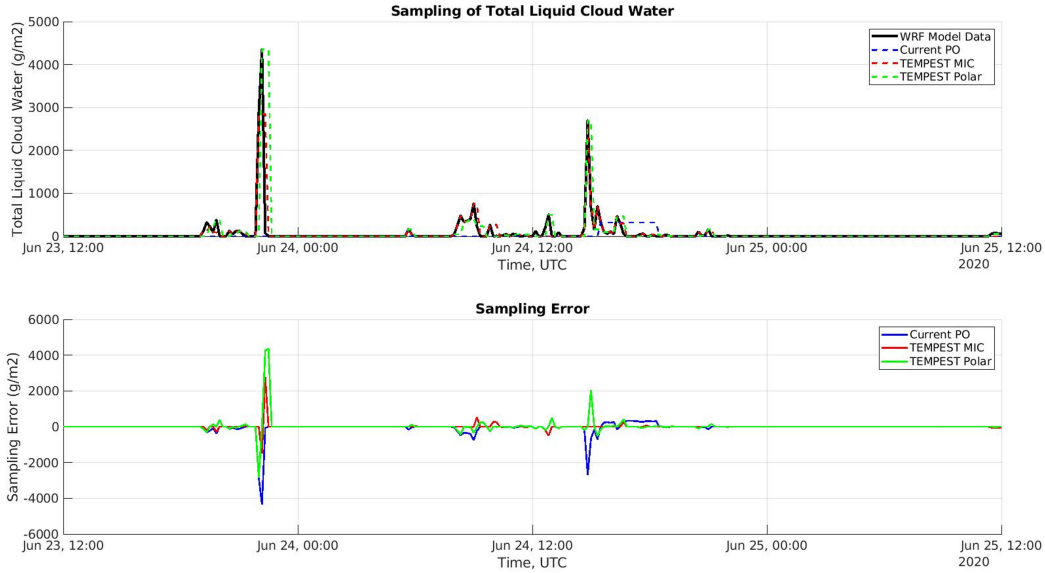

Fig. 8. (Upper panel) Temporal sampling of total liquid cloud water at Corpus Christi, TX. (Lower panel) The corresponding temporal representativeness error for the three constellation configurations studied.

way to decrease the mean revisit time is to increase the satellite orbital altitude. For example, four satellite subconstellations in low inclination, high-altitude orbits, with periods of 24 and 48 h, provide nearly continuous observation of Earth surface [16]. As mentioned previously, however, increasing the altitude also decreases the spatial resolution of the observations, so that such a constellation is of limited use for capturing storm dynamics or areas with strong temperature or water vapor gradients.

Another example of a remote sensing constellation providing short revisit times but limited coverage is the BlackSky [8] constellation. This constellation was designed to provide a mean revisit time of approximately 18 min over highly populated areas using a constellation of 60 LEO satellites in 10 orbital planes. Such a constellation would provide frequent observations of CONUS and Europe, but would provide no coverage for areas above 55° latitude. In contrast, the current polar orbiter constellation with the NOAA-20 and MetOp-C satellites in sun-synchronous, 820 km altitude orbits provides about 6 h mean revisit time over most of the Earth, but significantly oversamples the polar regions. A constellation deployed in a single orbital plane provides significantly a shorter mean revisit time over a range of latitudes near the orbital inclination. For that latitude band, however, periods of frequent observations are followed by relatively long gaps in coverage. For regions at lower latitudes than the zone of maximum coverage near the top and bottom of the orbit, observations are more evenly distributed over time. To provide more uniform temporal sampling over the Earth, the constellation should consist of satellites in multiple orbital planes with high inclination. If observing storm evolution and its associated dynamics is a high priority, then multiple lower inclination orbits should be selected to provide frequent coverage over regions with a high probability of those events. This is the case with the TROPICS mission, which chose to use three orbital planes at an inclination angle of 30°, to maximize temporal sampling in the latitude range where rapid intensification of hurricanes, typhoons, and tropical cyclones most frequently occurs, i.e., about 25° N and 25° S.

As discussed previously, an orbital altitude of 550 km provides approximately 10 km radiometer footprint size using a 12U CubeSat while providing an extended satellite lifetime and a reasonable swath width. For a cross-track scanning sensor with a maximum instrument scan angle of 50°, similar to that of the ATMS sensor [17], the swath width is ∼1400 km. Those parameters were used to simulate coverage for all constellations described below.

Constellation configurations were analyzed both for uniform sampling over the globe as well as a multi-inclination case for observing convective storm evolution, as described above. Results for two different satellite constellations simulated using the AGI Systems Tool Kit [18], [19] for a 5-day duration are shown here. The first constellation consists of 15 sun-synchronous orbital planes with ascending nodes distributed over a 180° span (Walker star pattern [20]). Each orbital plane contains four satellites (60 satellites total). The separation between orbit planes is chosen to maintain contiguous coverage near the equator. This configuration is subsequently referred to as the TEMPEST Polar constellation. The second constellation consists of groups of satellites in multiple orbital planes at inclination angles of 30°, 40°, 50°, 60°, and 70°. Each orbital inclination has two groups of satellites in separate orbital planes, for a total of 10 orbital planes, each populated with six satellites. This constellation configuration has a total of 60 satellites and is referred to as the TEMPEST Multi-Inclination Constellation (TEMPEST MIC). The coverage for these two constellations over a single orbital period is shown in Fig. 3. Calculations are based on the assumption that there is complete overlap between IFOVs, which is the case for the sampling time used. For reference, a constellation consisting of only the current NOAA-20 and MetOp-C polar orbiter constellation was also simulated.

As shown in Fig. 3 for the TEMPEST MIC constellation, the regions near latitudes of ± 30°, ± 40°, ± 50°, ± 60°, and ± 70° latitude might have more frequent sampling followed by relatively long gaps, while areas near the equator have more evenly distributed revisits.

Evaluating the mean revisit time as a function of latitude is one simple way to evaluate the temporal sampling performance of a constellation. Fig. 4 shows the mean revisit times for the current polar orbiter constellation, as well as the TEMPEST MIC and

TEMPEST Polar constellations, as a function of latitude. The simulation results show that the mean revisit time of the current polar orbiter constellation ranges from 4.0 to 6.5 h for latitudes between 60° N and 60° S. The enhanced TEMPEST Polar and TEMPEST MIC constellations reduce the mean revisit time to ∼20 and 10–15 min, respectively, for latitudes between 60° N and 60° S. Mean revisit time is a less useful metric, however, for scenarios in which a set of very frequent observations is followed by long periods with no observations (i.e., data gaps). In such a case, a relatively short mean revisit time does not adequately characterize the temporal sampling provided by the constellation.

Another way to examine temporal sampling of a satellite constellation is as a percentage of the time over which a given region is sampled within a specified revisit time. Fig. 5 shows the revisit time as a function of latitude for 25%, 50%, and 90% of the total observation time, i.e., 6, 12, and 21.5 h per day, respectively. For example, for the current polar orbiter constellation [Fig. 5(a)] at the equator, 50% of the time subsequent observations occur within 8 h, while 25% of the time they occur within ∼5 h. The TEMPEST MIC constellation exhibits much larger variability in revisit time. For the latitude range from 20° N to 40° N and 20° S to 40° S, 25% of the time the revisit time is within 5 min, while 50% of the time the revisit time is within 15 min for latitudes from 70° N to 70° S.

TEMPEST MIC also exhibits an increase in 50% revisit time (green curve) from 15 to almost 50 min near the equator, which is related to the fact that the coverage area with short revisit time, which occurs at the top and bottom of the orbit, for the lowest inclination orbit (30°) does not quite extend to the equator.

It is important to note that the TEMPEST MIC constellation does not provide coverage over polar regions with latitudes above 76°, although it is assumed that this region would be covered by existing and planned large operational satellites providing microwave observations from polar orbits.

For the TEMPEST Polar constellation, the 25%, 50%, and 90% threshold lines are very similar to each other for latitudes between 60° N and 60° S, demonstrating that TEMPEST Polar provides consistent and uniform revisit times of ∼20 min over most of the globe.

Perhaps the most intuitive way to visualize the advantages of the proposed constellations to track rapid atmospheric changes is to examine how each constellation samples variations in temperature, water vapor, and cloud properties for a specified location. Unfortunately, available global analysis datasets, including GEOS-5 and the ERA-5 reanalysis, do not provide sufficient temporal and spatial resolution. Therefore, results from WRF simulations with 10 min temporal and 12 km spatial resolution are shown here. The WRF simulation was run for a 2-day period from June 23, 2020 at 12:00 UTC to June 25, 2020 at 12:00 UTC over Corpus Christi, Texas. This simulation includes atmospheric conditions resulting in a severe thunderstorm and flood event on June 24, 2020 [21], thereby providing an example with high temporal variability. The corresponding temporal representativeness error for the three constellation configurations studied.

Time series of WRF-simulated water vapor and temperature at 700 mb pressure altitude are shown in Fig. 6, along with cloud LWP and cloud IWP over the 48-h period for Corpus Christi, TX. The black solid curve in Fig. 6(a) shows the simulated water vapor mixing ratio at 700 mb pressure altitude, which varies between 5 and 10.5 g/kg. The blue dashed curve shows this time series as sampled by the current polar orbiter constellation, while the red and green dashed curves show the time series as they would be sampled by the TEMPEST MIC and TEMPEST Polar constellations, respectively. The resulting sampling error, defined as the difference between the actual and sampled WRF model data, is shown in Fig. 6(b), indicating that the large decrease in water vapor at about 0:00 UTC on June 24, as well as the one at about 6:00 UTC on June 25, are not captured by the current polar-orbiting constellation, but would be captured by both the TEMPEST MIC and TEMPEST Polar constellations. The large increase in water vapor at 21:00 UTC on June 23 is also missed by the current polar orbiter constellation, but it would be captured by the TEMPEST MIC and TEMPEST Polar constellations, albeit with a 20–30 min time delay.

The corresponding time series for temperature at 700 mb in Fig. 7 shows that the enhanced TEMPEST MIC and TEMPEST Polar constellations have significantly lower temporal representativeness errors than the observations provided by the current polar orbiter constellation. For this case, the sampling error for both of the TEMPEST constellations is very similar. Corresponding time series of cloud LWP and cloud IWP are shown Figs. 8 and 9, respectively. For several storms during this period, the TEMPEST MIC constellation captures the highly variable cloud properties better than the TEMPEST Polar constellation. However, occasional gaps in the coverage by the TEMPEST MIC constellation cause it to miss some features that are captured by the more regular sampling provided by the TEMPEST Polar constellation (e.g., after midnight on June 24 and June 25).

V. Conclusion

The microwave radiometer on board the TEMPEST-D 6U CubeSat has demonstrated the capability of small, low-cost satellites, and sensors to perform science-quality all-sky observations for global forecasts and other science applications. An analysis of several previous studies along with WRF simulations indicates that capturing temporal variability of atmospheric temperature and water vapor requires temporal sampling of 1–2 h, while capturing the development of convective storms requires temporal sampling of about 20–30 min. To achieve this, two different constellations are considered and compared to the temporal sampling capabilities of the existing operational satellites providing microwave observations. The TEMPEST Polar constellation consists of 60-each 12U CubeSats in 15 different orbital planes, all of which are in sun-synchronous polar orbits. This constellation configuration provides the most evenly spaced global temporal sampling at ∼20 min, but cannot capture higher temporal variability associated with rapidly developing convective storm systems. The second constellation considered also employs 60 satellites, but in a range of different orbit inclinations at 30°, 40°, 50°, 60°, and 70°. This constellation, referred to as the TEMPEST MIC, exhibits occasional longer gaps between successive observations, but also provides periods with much more frequent revisit times of 5–10 min that enable this constellation approach to better capture storm development for applications like rapid intensification of hurricanes and typhoons.

This article advances the understanding of the dramatic improvement in temporal sampling of all-sky atmospheric conditions enabled by a constellation of low-cost CubeSat satellites with microwave radiometers, compared with the existing operational satellites providing microwave observations. Due to

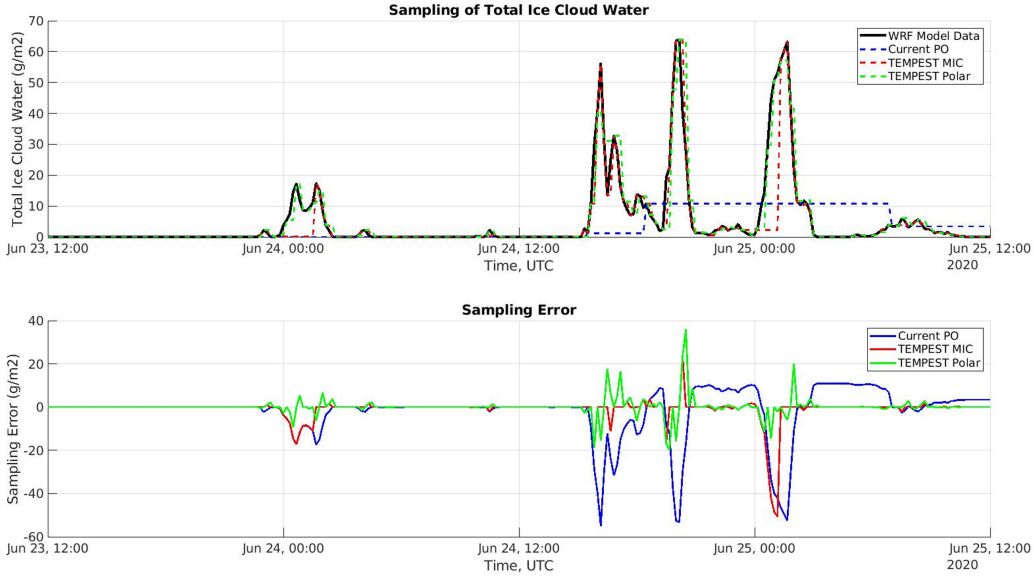

Fig. 9. (Upper panel) Temporal sampling of total ice cloud water at Corpus Christi, TX. (Lower panel) The corresponding temporal representativeness error for the three constellation configurations studied.

the improvement observed in the temporal representativeness of the state of the atmosphere, an expanded constellation of microwave sensors could improve global forecasts, particularly in regions with rapidly changing conditions, as well as provide valuable observations for research on the development of hurricanes and intense oceanic storms, as well as over regions of the globe with limited ground-based observations.

ACKNOWLEDGMENT

The authors would like to thank David Marks, Gabriela Bravo, David Spencer, and Patricia Weir at NOAA for contract management, as well as their encouragement and support. The authors would also like to thank Pamela Millar, Robert Bauer, and Sachinanda Babu for their supportive management of TEMPEST-D, a NASA SMD/ESD/Earth Venture Technology Demonstration Mission, as well as Jack Kaye and the late Gail Skofronick-Jackson of NASA SMD/ESD, for their support of TEMPEST-D mission science. The scientific results and conclusions, as well as any views or opinions expressed herein, are those of the author(s) and do not necessarily reflect those of NOAA or the Department of Commerce.

REFERENCES

[1] D. L. Wu et al., "IceCube: Spaceflight demonstration of 883-GHz cloud radiometer for future science," in *Proc. SPIE 11131, CubeSats SmallSats Remote Sens. III*, 2019, Art. no. 1113103.

[2] A. Crews et al., "Initial radiance validation of the microsized microwave atmospheric satellite-2A," *IEEE Trans. Geosci. Remote Sens.*, vol. 59, no. 4, pp. 2703–2714, Apr. 2021.

[3] S. Padmanabhan *et al.*, "TEMPEST-D radiometer: Instrument description and prelaunch calibration," *IEEE Trans. Geosci. Remote Sens.*, vol. 59, no. 12, pp. 10213–10226, Dec. 2021.

[4] W. Berg *et al.*, "Calibration and validation of the TEMPEST-D cubesat radiometer," *IEEE Trans. Geosci. Remote Sens.*, vol. 59, no. 6, pp. 4904–4914, Jun. 2021.

[5] W. J. Blackwell *et al.*, "An overview of the TROPICS NASA earth venture mission," *Quart. J. Roy. Meteorol. Soc.*, vol. 144, no. 1, pp. 16–26, Mar. 2018.

[6] K. K. Kramer, S. V. Fridma, and L. J. Nickisch, "An evaluation of spire radio occultation data in assimilative ionospheric model GPSII and validation by ionosonde measurements," in *Proc. XXXIIIrd General Assembly Sci. Symp. Int. Union Radio Sci.*, 2020, pp. 1–4.

[7] Spire Global Inc., "Earth surface observations using GNSS bistatic radar (reflectometry) on spire's constellation of cubesats," in *7th International Colloquium on Scientific and Fundamental Aspects of GNSS*. Zurich, Switzerland: Danish Meteorological Institute, 2019.

[8] Smallsat constellations. satelliteobservation.net, Accessed: May 10, 2021. [Online]. Available: https://satelliteobservation.net/2017/02/11/smallsat-constellations/

[9] The National Severe Storms Laboratory. SEVERE WEATHER 101: Thunderstorm Types. nssl.noaa.gov, Accessed: May 10, 2021. [Online]. Available: https://www.nssl.noaa.gov/education/svrwx101/thunderstorms/types/

[10] J. S. Bendat and A. G. Pirsol, *Random Data Analysis and Measurement Procedures*, 1st ed. New York, NY, USA: Willey, 1971.

[11] S. Steinke *et al.*, "Assessment of small-scale integrated water vapour variability during HOPE," *Atmos. Chem. Phys.*, vol. 15, no. 5, pp. 2675–2692, Mar. 2015.

[12] H. Vogelmann, R. Sussmann, T. Trickl, and A. Reichert, "Spatiotemporal variability of water vapor investigated using lidar and FTIR vertical soundings above the zugspitze," *Atmos. Chem. Phys.*, vol. 15, no. 6, pp. 3135–3148, Mar. 2015.

[13] S. Bley, H. Deneke, and F. Senf, "Meteosat-based characterization of the spatiotemporal evolution of warm convective cloud fields over central Europe," *J. Appl. Meteorol. Climatol.*, vol. 55, no. 10, pp. 2181–2195, Oct. 2016.

[14] Advanced Research WRF (ARW) Modeling System (Version 3.9). Accessed: May 10, 2021. [Online]. Available: https://www2.mmm.ucar.edu/wrf/users/docs/user_guide_V3.9/users_guide_chap5.htm

[15] "National centers for environmental prediction/national weather Service/NOAA/U.S. department of commerce," (Updated daily), NCEP GFS 0.25 Degree Global Forecast Grids Historical Archive.

[16] L. A. Singh *et al.*, "Low cost satellite constellations for nearly continuous global coverage," *Nature Commun.*, vol. 11, Jan. 2020, Art. no. 200.

[17] H. Yang, F. Weng, and K. Anderson, "Estimation of ATMS antenna emission from cold space observations," *IEEE Trans. Geosci. Remote Sens.*, vol. 54, no. 8, pp. 4479–4487, Aug. 2016.

[18] AGI Systems Tool Kit (STK). Accessed: May 10, 2021. [Online]. Available: https://www.agi.com/products/stk

[19] Satellite Constellation Design. AGI. Accessed: Sep. 24, 2021. [Online]. Available: https://www.agi.com/resources/videos/satellite-constellation-design

[20] J. G. Walker, "Satellite constellations," *J. Brit. Interplanetary Soc.*, vol. 37, pp. 559–571, 1984.
[21] Wednesday afternoon thunderstorms leave residents without power and roads with high water, Kiiitv.com. Accessed: May 10, 2021. [Online]. Available: https://www.kiiitv.com/article/news/thousands-of-residents-in-corpus-christi-flour-bluff-and-surrounding-areas-experiencing-power-outage/503-4ec91ad2-172e-49a3-abbd-43013530f181

Yuriy V. Goncharenko (Member, IEEE) received the B.S. and M.S. degrees in electrical engineering from Kharkov National Polytechnic University, Kharkiv, Ukraine, in 1998 and 1999, respectively, and the Ph.D. degree in radiophysics from the Institute for Radiophysics and Electronics NAS of Ukraine, Kharkiv, Ukraine, in 2006.

From 2012 to 2013, he was a Fulbright Scholar with Applied Physics Laboratory, University of Washington, Seattle, WA, USA, where he focused on airborne synthetic aperture radars for remote sensing of the sea surface. He also worked with the University of Birmingham, Birmingham, U.K., on the design of signal processing algorithms for ultraprecise quantum gravity sensors. He is currently with the Microwave Systems Laboratory, Colorado State University, Fort Collins, CO, USA. His research interests include the design and implementation of calibration, signal processing, and target detection techniques.

Wesley Berg (Member, IEEE) received the B.S., M.S., and Ph.D. degrees in aerospace engineering from the University of Colorado, Boulder, CO, USA, in 1988, 1989, and 1993, respectively.

He is currently a Senior Research Scientist with the Department of Atmospheric Science, Colorado State University, Fort Collins, CO, USA. He worked previously with the Cooperative Institute for Research in Environmental Science within NOAA's Environmental Research Laboratories. His research interests include satellite remote sensing of precipitation and other hydrologic parameters with a focus on instrument calibration and the development and analysis of satellite retrievals for long-term climate applications.

Steven C. Reising (Senior Member, IEEE) received the B.S.E.E. (*magna cum laude*) and M.S.E.E. degrees in electrical engineering from Washington University in St. Louis, Saint Louis, MO, USA, in 1989 and 1991, respectively, and the Ph.D. degree in electrical engineering from Stanford University, Stanford, CA, USA, in 1998.

He served as an Assistant Professor in electrical and computer engineering with the University of Massachusetts Amherst, Amherst, MA, USA, from 1998 to 2004, where he received tenure. He was a Visiting Faculty Member with the University of Paris VI, *Université Pierre et Marie Curie*, Paris, France, during the first half of 2014. He joined Colorado State University, Fort Collins, CO, USA, in 2004, where he served as an Associate Professor from 2004 to 2011 and has been a Full Professor in electrical and computer engineering since July 2011. His research interests include broad range of remote sensing disciplines, including microwave remote sensing of the Earth's atmosphere and oceans from airborne platforms, small satellites and CubeSats; the design and development of radiometer systems from microwave to submillimeter-wave and THz frequencies (18–850 GHz); lidar systems for sensing temperature and winds in the middle and upper atmosphere; and lightning-ionosphere interactions and atmospheric electrodynamics.

Prof. Reising has been the Principal Investigator of 18 grants from NASA, NOAA, National Science Foundation (NSF), Department of Defense, Office of Naval Research, NPOESS, European Space Agency, Ball Aerospace, and FIRST RF Corporation. He has served as a Principal Faculty Advisor for 16 M.S./Ph.D. students who have completed their degrees and are currently employed as professors, engineers, and researchers in universities, industry, and government laboratories. He was the recipient of the NSF CAREER Award (in the areas of physical and mesoscale dynamic meteorology from 2003 to 2008, and the Office of Naval Research Young Investigator Program Award for passive microwave remote sensing of the oceans from 2000 to 2003. He currently serves as the Secretary of the IEEE Geoscience and Remote Sensing Society (GRSS). He previously served as the Chair of the ad-hoc Committee for Intersocietal Relations (2019–2020) and as an elected Administrative Committee (AdCom) Member of the IEEE GRSS from 2003 to 2020. He also previously served as an elected AdCom Member of the IEEE Microwave Theory and Techniques Society (MTT-S) from 2014 to 2019. He served the IEEE as MTT-S Inter-Society Committee Chair from 2015 to 2018, GRSS Vice-President of Information Resources from 2011 to 2018, and the GRSS Vice-President of Technical Activities from 2008 to 2010. He was a founding member of the *IEEE Geoscience and Remote Sensing Letters* Editorial Board and served as an Associate Editor from 2004 to 2013. He is a Guest Editor of three Special Issues and one Special Section of the *IEEE Transactions on Geoscience and Remote Sensing*. He served as the Immediate Past Chair of the U.S. National Committee of the International Union of Radio Science (URSI) from 2015 to 2017, the Chair from 2012 to 2014, and the Secretary from 2009 to 2011, of all 10 URSI Commissions. He is a member of URSI Commissions F, G, and H, the American Meteorological Society, the American Geophysical Union, the American Association for the Advancement of Science, Tau Beta Pi, and Eta Kappa Nu.

Flavio Iturbide-Sanchez (Senior Member, IEEE) received the B.S.E.E degree in electronics engineering from Autonomous Metropolitan University, Mexico City, Mexico, in 1999, the M.S.E.E. degree in electrical engineering from the Advanced Studies and Research Center, National Polytechnic Institute, Mexico City, Mexico, in 2001, and the Ph.D. degree in electrical engineering from the University of Massachusetts, Amherst, MA, USA, in 2007.

From 2001 to 2005, he was a Research Assistant with the Microwave Remote Sensing Laboratory, University of Massachusetts, where he was involved in the design, development, and characterization of highly integrated multichip modules and microwave circuits for low-noise, low-power consumption, high-gain, and high-stability microwave radiometers. From 2005 to 2007, he was with the Microwave Systems Laboratory, Colorado State University, Fort Collins, CO, USA, focusing on the demonstration of a low-cost and power-efficient compact microwave radiometer for humidity profiling. From 2008 to 2018, he supported the development of operational physical retrieval systems that employ hyperspectral-infrared and microwave observations implemented for the Polar Operational Environmental Satellites Project and the Joint Polar Satellite System (JPSS). He has been a Physical Scientist with NOAA/NESDIS/Center for Satellite Applications and Research, College Park, MD, USA, since 2018, where he has led the calibration and validation of the JPSS Cross-Track Infrared Sounder instruments and supports the planning of the next generation of NOAA infrared and microwave sounders. His research interests include satellite remote sensing, satellite data assimilation, inverse theory applied to geoscience fields, weather forecasting, earth system science, small satellites, and the design of radiometer systems for earth observations based on emerging technologies. His Ph.D. research interests include miniaturization, development, calibration, and performance assessment of low-cost and power-efficient microwave radiometers for remote sensing applications.

V. Chandrasekar (Fellow, IEEE) received the bachelor's degree in electrical engineering from IIT Kharagpur, Kharagpur, India, in 1981, and the Ph.D. degree in electrical engineering from Colorado State University (CSU), Fort Collins, CO, USA, in 1986.

He is currently a University Distinguished Professor with CSU. He has been actively involved with research and application of weather radar systems. He has coauthored 2 textbooks, 5 general books, and about 200 journal articles.

Prof. Chandrasekar is an Elected Fellow of the International Union of Radio Science (URSI), NOAA/CIRA, and the American Meteorological Society. He served as the Editor-in-Chief for the *Journal of Atmospheric and Oceanic Technology*. He serves as the Chair for Commission F URSI. He was a recipient of numerous awards, including the NASA Technical Contribution Award, the NASA Group Achievement Award, the NASA Robert H. Goddard Exceptional Achievement Award, the Outstanding Advisor Award, the CSU Innovations Award, the IEEE GRSS Education Award, the NOAA/NWS Directors Medal of Excellence, and the Knight of the Government of Finland. He served as the General Chair for the IEEE IGARSS'06 Symposium.